JLB

Article

Cholesterol-dependent cytolysins induce rapid release of mature IL-1β from murine macrophages in a NLRP3 inflammasome and cathepsin B-dependent manner

Jessica Chu, L. Michael Thomas,* Simon C. Watkins,[†,‡] Luigi Franchi,[§] Gabriel Núñez,[§] and Russell D. Salter[†,1]*

*Immunology Graduate Program and Departments of [†]Cell Biology and Physiology and [‡]Immunology, University of Pittsburgh School of Medicine, Pittsburgh, Pennsylvania, USA; and [§]Department of Pathology and Comprehensive Cancer Center, University of Michigan Medical School, Ann Arbor, Michigan, USA

RECEIVED MARCH 12, 2009; REVISED JULY 1, 2009; ACCEPTED JULY 3, 2009. DOI: 10.1189/jlb.0309164

ABSTRACT

CDC are exotoxins secreted by many Gram-positive bacteria that bind cholesterol and oligomerize to form pores in eukaryotic cell membranes. We demonstrate that CDC TLO induces caspase-1 cleavage and the rapid release of IL-1β from LPS-primed murine BMDM. IL-1β secretion depends on functional toxin pore formation, as free cholesterol, which prevents TLO binding to cell membranes, blocks the cytokine release. Secretion of the mature forms of IL-1β and caspase-1 occurs only at lower TLO doses, whereas at a higher concentration, cells release the biologically inactive proforms. IL-1β release at a low TLO dose requires potassium efflux, calcium influx, and the activities of calcium-independent PLA_2, caspase-1, and cathepsin B. Additionally, mature IL-1β release induced by a low TLO dose is dependent on the NLRP3 inflammasome, and pro-IL-1β release induced by a high TLO dose occurs independently of NLRP3. These results further elucidate a mechanism of CDC-induced IL-1β release and suggest a novel, immune evasion strategy in which IL-1β-containing macrophages might release primarily inactive cytokine following exposure to high doses of these toxins. *J. Leukoc. Biol.* 86: 1227–1238; 2009.

Introduction

CDC are a class of protein exotoxins that are secreted by over 20 species of Gram-positive bacteria [1, 2]. Individual subunits bind to cholesterol in eukaryotic cell membranes and oligomerize to form transmembrane pores up to 30 nm in size [1–5]. Forty to 80 CDC monomers assemble into a pre-pore complex before membrane insertion and final pore conversion, which results in osmotic imbalance that may lead to cell death. Mice injected i.v. with 100 pmol purified forms of several different CDC underwent almost immediate death [6], demonstrating the potent biological activities of these toxins. PLY-deficient Streptococcus *pneumoniae* have reduced virulence in mice, supporting a potential role for such toxins in bacterial pathogenesis [7, 8]. In contrast, immunization of mice with ALO or a genetic toxoid does not protect against *Bacillus anthracis* infection [9], suggesting that for some CDC-bearing pathogens, the toxin plays a less-important role. It should be noted that at least one CDC, LLO, has a specialized role in allowing escape of *Listeria* from the phagosome into the cytosol and is maximally active at acidic pH [10, 11]. Although CDC such as ALO can substitute for LLO when manipulated experimentally [12], most CDC do not show a marked pH dependence and are believed to function primarily extracellularly following secretion by bacteria, acting on adjacent cells in the infected host.

Although all eukaryotic cells are susceptible to toxin-induced lysis, the amounts required for killing vary widely between cell types [13]. This may be a result of a differential ability of distinct cell types to repair membranes damaged by pores. Evidence for membrane repair after toxin damage has been obtained by measuring cytoplasmic ATP levels, which decrease drastically after exposure to sublethal concentrations of toxin before a return to normal levels [14, 15]. At higher lytic levels of toxin, recovery of ATP levels is not observed. The mechanism of repair involves removal of pores from the plasma membrane via an endocytic process [16]. Cells that have been exposed to sublytic doses of toxin and then recover

Abbreviations: Ac-YVAD-cmk=Ac-Tyr-Val-Ala-Asp-chloromethylketone, ALO=anthrolysin O, BEL=bromoenol lactone, BMDM=bone marrow-derived macrophage(s), CDC=cholesterol-dependent cytolysin(s), $iPLA_2$=calcium-independent phospholipase A_2, KO=knockout, LDH=lactate dehydrogenase, LLO=listeriolysin O, NLR=Nod-like receptor, NLRC4=NOD-like receptor family caspase-associated recruitment domain-containing 4, NLRP3=NOD-like receptor family pyrin domain-containing 3, PFT=pore-forming toxin, PLA_2=phospholipase A_2, PLY=pneumolysin, SLO=streptolysin O, TLO=tetanolysin O, TMB=3,3′,5,5′-tetramethyl benzidine, Z-FF-fmk=benzyloxycarbonyl-Phe-Phe-fluoromethylketone, z-VAD-fmk=benzyloxycarbonyl Val-Ala-Asp-fluoromethylketone

1. Correspondence: University of Pittsburgh School of Medicine, E1052 BST, 200 Lothrop St., Pittsburgh, PA 15213, USA. E-mail: rds@pitt.edu

may be altered phenotypically, and there are numerous examples of such sublethal effects of CDC [1].

In immune cells, exposure to CDC toxins at concentrations that are not lytic have been observed to induce release of cytokines and chemokines [1, 17], and cytokine and chemokine secretion is particularly important for the recruitment and activation of inflammatory immune cells to the local site of bacterial infection. One major cytokine family that plays a role in the inflammation process is the IL-1 family. Included in this family are IL-1α and IL-1β, which are released upon interaction of cells with CDC. Specifically, LLO induces the release of IL-1α from murine macrophages [18], and SLO and PLY cause the secretion of IL-1β from human monocytes [19, 20]. The mechanism by which CDC induce release of IL-1 has not been fully characterized to date.

IL-1α and IL-1β, as well as IL-18 and IL-33, are stored inside cells, such as macrophages and dendritic cells, as precursors whose synthesis is induced by exposure to TLR ligands (signal 1) [21]. Unlike many other cytokines, efficient release requires exposure of cells to a second stimulus to initiate processing and the nonclassical secretion of the active cytokine. The second stimuli lead to the activation of inflammasome complexes, which consist of members of the NLR family for the activation of inflammatory caspases such as caspase-1 (for a review, see refs. [22–24]). The best-known examples of these caspase-1-activating platforms are the NLRP1, NLRP3, and NLRC4 inflammasomes, which lead to the processing of the pro-form of IL-1β to its mature form. To date, multiple second stimuli for these various inflammasomes have been identified (for a review, see ref. [23]), and select ones will be discussed below.

One of the best-studied second stimuli is ATP, which acts by binding to the purinergic receptor $P2X_7$, initiating calcium influx and potassium efflux via its ion channel function [25]. Calcium is also released from intracellular stores during this process and contributes to cytokine release [26]. Potassium efflux leads to activation of calcium-independent phospholipase ($iPLA_2$) [27] and the NLRP3 inflammasome, which contains dimeric caspase-1, adaptor apoptosis-associated speck-like protein containing a C-terminal caspase recruitment domain, and NLRP3 (also known as cryopyrin or NALP3) [28]. Activation of this inflammasome leads to cleavage of caspase-1, which has been shown to cleave inactive pro-IL-1β to generate active, mature IL-1β for release from the cell. Additionally, $P2X_7$ activation causes recruitment of pannexin-1 protein to form a nonselective pore for passage of molecules up to ~900 Da across membranes [29, 30]. This pannexin-1 pore is thought to allow ion fluxes as well as the passage of bacterial products from inside endosomes or phagosomes into the cytosol for the subsequent activation of one or more inflammasome complexes [31].

An additional stimulus that can activate the NLRP3 inflammasome and initiate IL-1β release is potassium ionophore nigericin, which exerts its effects primarily through a potassium efflux mechanism [32]. Much like ATP, it also relies on the activity of caspase-1 but acts independently of $P2X_7$ [33]. Other stimuli inducing IL-1β release from myeloid cells through a NLRP3 and caspase-1-dependent mechanism include uric acid crystals [34], silica crystals [35, 36], aluminum salt crystals [35], and amyloid-β fibrils [37]. All of these can be phagocytosed by macrophages and appear to disrupt lysosomes, resulting in leakage of their contents into the cytosol [38]. It was reported recently that cathepsin B is required for release of IL-1β following stimulation with silica crystals, aluminum salt crystals, or amyloid-β [35, 37], which supports a scenario in which mislocalized cathepsin B is involved in aspects of NLRP3 inflammasome activation or subsequent IL-1β release. In fact, other groups have shown that cathepsin B activates caspase-11, which in turn, acts as an upstream activator of caspase-1 [39, 40].

In this report, we describe the mechanism of rapid IL-1β release after exposure of LPS-primed murine BMDM to the CDC TLO. Cytokine release occurs maximally within 2 h of initial treatment with little additional release occurring by 20 h post-treatment. Although TLO-induced IL-1β secretion is dependent on functional toxin pore formation, this alone is not sufficient for the processing and secretion of IL-1β. Lower TLO doses are required for release of mature IL-1β, as well as for the cleavage and release of mature caspase-1, as opposed to higher doses that enable the release of the inactive pro-IL-1β. Similarly to ATP and nigericin, TLO-induced release is dependent on potassium efflux, calcium influx, and the activities of $iPLA_2$, caspase-1, and cathepsin B, as determined by pharmacological inhibition. Moreover, TLO-induced release of mature IL-1β is dependent on the NLRP3 inflammasome and independent of the NLRC4 inflammasome, based on studies using BMDM deficient in NLRP3 or NLRC4. In summary, we further elucidate a mechanism for CDC-induced release of IL-1β.

MATERIALS AND METHODS

Reagents

TLO was obtained from Biomol International (Plymouth Meeting, PA, USA). Toxin was reduced with 10 mM DTT (Sigma-Aldrich, St. Louis, MO, USA) for 10 min, 37°C, before use, unless indicated, and untreated control samples were incubated in the same buffer lacking toxin. ATP, nigericin, LPS, cholesterol, and pepstatin A were purchased from Sigma-Aldrich; z-VAD-fmk/pan-caspase inhibitor VI, BAPTA-AM, Z-FF-fmk/cathepsin L inhibitor I, and CA-074 Me/cathepsin B inhibitor IV from EMD Biosciences (Gibbstown, NJ, USA); Ac-YVAD-cmk/caspase-1 inhibitor II and BEL from Axxora, LLC (San Diego, CA, USA); and Triton X-100 from Fisher Scientific (Pittsburgh, PA, USA). Purified anti-mouse IL-1α and IL-1β capture antibodies, biotin-conjugated anti-mouse IL-1α and IL-1β detection antibodies, and rIL-1α were acquired from eBioscience (San Diego, CA, USA). Purified and biotin-conjugated anti-mouse TNF-α antibodies, rTNF-α, rIL-1β, avidin-HRP, and TMB were obtained from Biolegend (San Diego, CA, USA).

BMDM preparation

The following protocol was adapted from ref. [41]. Tibiae and femurs from wild-type (gifts from Dr. Lisa Borghesi, University of Pittsburgh, PA, USA), $NLRP3^{-/-}$, or $NLRC4^{-/-}$ C57BL/6 mice were collected. BM cells were extracted using a 27-gauge needle and passed through a 21-gauge needle to obtain a homogenous mixture. Cells were plated in petri dishes (Day 1) in DMEM (Mediatech, Inc., Herndon, VA, USA), supplemented with 20% Gemcell™ FBS (Gemini Bio-Products, West Sacramento, CA, USA), 2 mM L-glutamine, 500 U penicillin/500 μg streptomycin (Lonza, Inc., Walkersville, MD, USA), 1 mM sodium pyruvate (MP Biomedicals, Solon, OH, USA), and 30% L cell supernatant, which was generated by incubating L

cell fibroblasts (CCL-1 from American Type Culture Collection, Manassas, VA, USA) in DMEM, supplemented with 10% Gemcell™ FBS, 2 mM L-glutamine, 500 U penicillin/500 μg streptomycin, 1× nonessential amino acids (Irvine Scientific, Santa Ana, CA, USA), and 1 mM sodium pyruvate until confluent. Supernatant was collected and filtered through a 0.22-um filter. Differentiation media for BMDM were changed every 3–4 days, and BMDM were used for experiments on Days 8–22. For experiments, BMDM were cultured in IMDM (Lonza, Inc.) containing 10% Gemcell™ FBS, 2 mM L-glutamine, and 500 U penicillin/500 μg streptomycin.

Western blotting

BMDM (2×10^6; plated the day before) were treated for 4 h in serum-containing IMDM with 1 μg/ml LPS and various concentrations of TLO or were left untreated. In some cases, following LPS priming, BMDM were incubated for 30 min in serum-free media with DTT control buffer, various doses of TLO, 3 mM ATP, 20 μM nigericin, or 1% Triton X-100. Where indicated, 1 ml supernatants were collected and TCA/cholic acid-precipitated as described by Qu and colleagues [42]. Cells were harvested, washed, and lysed or lysed directly in wells with Nonidet P-40 lysis buffer containing a protease inhibitor cocktail (Sigma-Aldrich). Bradford assay (Bio-Rad, Hercules, CA, USA) was conducted to determine protein concentration of lysates, and 20–50 μg protein lysate was run on SDS-PAGE gels along with concentrated supernatants (where indicated). Proteins were transferred to polyvinylidene difluoride membrane using Towbin buffer transfer or the iBlot™ system (Invitrogen, Carlsbad, CA, USA) and probed for IL-1β with mouse anti-IL-1β primary antibody (3ZD; National Cancer Institute Biological Resources Branch, Frederick Cancer Research and Development Center, Frederick, MD, USA) and goat anti-mouse IgG-HRP secondary antibody (Santa Cruz Biotechnology, Santa Cruz, CA, USA) using the SNAP i.d.™ system (Millipore, Bedford, MA, USA). Membranes were also probed for caspase-1 with rabbit anti-caspase-1 primary antibody and donkey anti-rabbit IgG-HRP secondary antibody (Biolegend). In some cases, the same blot was stripped with Restore Plus Western blot stripping buffer (Thermo Scientific, Rockville, MD, USA), according to the manufacturer's protocol, and reprobed with rabbit anti-β-actin primary antibody (Biolegend) and donkey anti-rabbit IgG-HRP secondary antibody. Western blotting luminol reagent (Santa Cruz Biotechnology) was applied, and membranes were imaged and analyzed (densitometry) with Kodak Image Station 4000MM (Molecular Imaging Systems, Carestream Health, Inc., Rochester, NY, USA). The net intensity of a single IL-1β protein band in a supernatant sample is expressed as a percentage of the total net intensities of IL-1β protein bands in all of the supernatant samples for a given blot.

Preparation of ELISA supernatants

BMDM (1×10^5) were plated/well of 24-well plates overnight in IMDM. The next day, the spent media were removed, and BMDM were primed with 1 ug/ml LPS for 4 h. LPS was then removed, and 300 μl of the indicated treatments was added for the indicated times. As TLO pore-forming activity is inhibited by free cholesterol present in FBS, TLO treatments were added in IMDM lacking FBS for 5 min, followed by addition of 10% FBS. Cholesterol inhibition of TLO activity was conducted by pre-mixing 1 ug/ml free cholesterol with TLO before addition to cells. For all other inhibitor experiments, inhibitors were preincubated with BMDM for 1 h after LPS removal prior to the addition of TLO, ATP, or nigericin. Inhibitors were prepared in serum-free IMDM containing 0.01% BSA. Supernatants were collected, centrifuged 10,000 rpm for 10 min, and stored at –20°C before analysis by ELISA.

ELISA

High-bind polystyrene 96-well plates (Greiner Bio-One, Monroe, NC, USA) were coated with 100 μl/well 1 μg/ml purified anti-mouse IL-1α, 4 μg/ml purified anti-mouse IL-1β, or 1× purified anti-mouse TNF-α capture antibody overnight. Wells were washed three times with 200 μl/well wash buffer (0.05% Tween® 20 in PBS), and this step was repeated in between each of the following incubations: 200 μl/well filtered 1% BSA in PBS for 1 h at room temperature; 100 μl/well standards or supernatant samples for 2 h at room temperature; 100 μl/well 1 μg/ml biotinylated anti-mouse IL-1α, 6 μg/ml biotinylated anti-mouse IL-1β, or 1× biotinylated anti-mouse TNF-α detection antibody for 1 h at room temperature; 100 μl/well 1:5000 avidin-HRP for 30 min at room temperature; 100 μl/well TMB substrate for 10 min (IL-1α, TNF-α) or 20 min (IL-1β) at room temperature; and 50 μl/well 1 M sulfuric acid to stop the reaction. OD values were read at 450 nm with a 570-nm subtracted correction using a BioTek® PowerWave™ XS microplate spectrophotometer, and data were analyzed using Gen5™ data analysis software (BioTek® Instruments, Inc. Winooski, VT, USA).

LDH release assay

BMDM (4.5×10^5) were plated/35 mm dish overnight in IMDM. The next day, spent media were removed, and BMDM were treated with 1 ug/ml LPS for 4 h. Cells were then washed with PBS and incubated for 30 min with DTT control buffer or various TLO concentrations in phenol red-free IMDM. Triton X-100 (1%) was used as a control of complete cell lysis and maximal LDH release. Supernatants were collected and assayed in duplicate for LDH content using the LDH cytotoxicity assay kit from Cayman Chemical Co. (Ann Arbor, MI, USA). Percent cytotoxicity was calculated as follows: [(mean OD value of experimental sample–mean blank OD)/(mean OD value of Triton X-100 control sample–mean blank OD)] × 100. BMDM from these experiments were harvested from dishes using CellStripper™ (Mediatech, Inc.) and stained with 5 μM YO-PRO-1 dye (Invitrogen) before analysis using a BD Biosciences (San Jose, CA, USA) LSR II flow cytometer and accompanying FACSdiva™ software. BMDM were also stained with YO-PRO-1 after 5 min of DTT control buffer or TLO treatments.

Cy5 labeling of toxin

A monofunctional N-hydroxysuccinimide-ester Cy5 (GE Healthcare, Piscataway, NJ, USA) vial was resuspended in 20 μl PBS and diluted 1:100. TLO (2.5 μg; 2.5 μl) or 2.5 μg BSA control (2.5 μl) was labeled with 0.5 μl PBS (control, unlabeled TLO) or 0.5 μl 1:100 Cy5 (TLO-Cy5) for 10 min at room temperature in the dark. To quench each reaction, 2.5 μg BSA was added and incubated for 10 min at room temperature in the dark.

Toxin binding and pore formation flow cytometry assay

BMDM (4.5×10^5) were plated/35 mm petri dish overnight in IMDM. The next day, spent media were removed, and BMDM were treated with 1 ug/ml LPS for 4 h. LPS was then removed, and 1 ml each indicated inhibitor was added for 1 h. Inhibitors were prepared in serum-free IMDM containing 0.01% BSA. Then, TLO, TLO-Cy5, or BSA-Cy5 was added to cells in the presence or absence of 1 μg/ml cholesterol for 5 min. Cells were harvested from dishes and stained with 5 μM YO-PRO-1 dye before analysis by flow cytometry. FlowJo (Tree Star, Inc., Ashland, OR, USA) was used for data analysis. A similar protocol was followed for BMDM treated with unlabeled TLO in the presence or absence of 1 μg/ml cholesterol.

Live cell microscopy

BMDM (1×10^5) were plated/35 mm collagen-coated glass-bottom culture dish (MatTek Corp., Ashland, MA, USA) overnight in IMDM. The next day, cells were primed with 1 μg/ml LPS for 4 h. Cells were washed with serum-free IMDM and incubated for 15 min with 0.5 μM LysoTracker™ Green in serum-free IMDM. BMDM were treated with a final concentration of 1.8 nM TLO-Cy5 in serum-free media. In indicated experiments, TLO-Cy5 was preincubated with 1 μg/ml cholesterol before addition to cells. Live cell imaging was performed using a Nikon TI inverted microscope with a 60× 1.49-NA oil immersion optic, a NikonPiezo-driven XYZ stage, a Prairie Sweptfield confocal head, and a Prairie Technology (Madison, WI, USA) laser bench. Images were collected using a QuantEM back-thinned 512B camera (Photometrics, Tucson, AZ, USA). Cells were maintained at 37°C in the microscope with a Tokai Hit environmental stage (Tokyo, Japan). Software control of the microscope was with Elements (Nikon,

Melville, NY, USA). Data analysis was performed using Metamorph software.

Graphical and statistical analysis

All graphing analyses were completed using Microsoft Excel (Microsoft, Redmond, WA, USA). Statistical analysis (Student's paired *t*-test) was conducted with GraphPad Prism (GraphPad Software, Inc., San Diego, CA, USA). *P* values were denoted as follows: *, $P \leq 0.05$; **, $P \leq 0.01$; $P > 0.05$ = not significant.

RESULTS

TLO-induced IL-1β release occurs via a mechanism distinct from TLR activation

Previous studies reporting IL-1 induction by CDC did not fully characterize the mechanism involved. As CDC have been reported to activate TLR4 [43–47], we considered whether nonlytic doses of TLO could prime BMDM to synthesize pro-IL-1β similarly to LPS. Release of IL-1β might be expected to occur at low levels following such treatment, particularly if some cell death occurred over the time course of the experiment. To test this, Western blotting was first used to measure pro-IL-1β levels in lysates of cells exposed to varying doses of TLO or 1 μg/ml LPS. At all concentrations of TLO tested, after a 4-h period, no pro-IL-1β could be detected, and large amounts were induced by LPS (**Fig. 1**). In addition, there was little to no detectable release of IL-1β from TLO-primed cells over this 4-h time period, as measured by a sensitive ELISA assay to test culture supernatants (detection limit, 16 pg/ml; data not shown). Thus, TLO cannot replace LPS for the priming of cells to synthesize pro-IL-1β.

We next tested if LPS-primed cells could release IL-1 after exposure to TLO. A time course of IL-1β (**Fig. 2A**) as well as IL-1α (Fig. 2B) release demonstrates the rapid rates at which these cytokines are exported after TLO exposure, with near-maximal secretion seen by 2 h. Nonprimed BMDM, as well as cells exposed to TLO for 4 h without LPS, could not be induced to secrete IL-1β following addition of TLO, ATP, or nigericin (data not shown). This rapid secretion contrasts to the release of another proinflammatory cytokine, TNF-α, from LPS-primed BMDM, which have been exposed to control buffer, TLO, ATP, or nigericin for up to 2 h (Fig. 2C). LPS priming induces background levels of TNF-α, as seen for the control, but additional treatment with TLO, ATP, or nigericin does not raise these levels significantly above background. These results are consistent with TLO acting to induce rapid release of IL-1β and IL-1α and suggest that this occurs independently of TLR activation. The kinetics of the response was similar to those for ATP and nigericin, suggesting possible mechanistic similarities.

Pore formation is required for TLO-induced IL-1β secretion

To further address the mechanism of CDC-induced cytokine release, we determined whether TLO pore formation was required to induce IL-1β release. Free cholesterol was added to TLO at a concentration shown previously to inhibit its ability to bind cholesterol on cell membranes and subsequently form pores [13]. Cholesterol-inhibited TLO was not able to induce IL-1β release from BMDM (**Fig. 3**). To confirm that pore formation was blocked under these conditions, uptake of YO-PRO-1 dye, which does not cross intact cell membranes but readily enters permeabilized cells [29, 48], was measured (Fig. 3, inset). Thus, TLO-induced pore formation is required for the release of IL-1β.

Lower TLO doses are required for the release of mature IL-1β

A straightforward explanation for the above results might be that TLO exposure could passively lead to release of IL-1β from BMDM through toxin-induced pores. To begin to test this possibility, toxin-induced pore formation in BMDM membranes, measured by YO-PRO-1 uptake, was compared with toxin-induced, passive spilling of intracellular contents, as measured by LDH release. BMDM became perforated within 5 min of treatment by even the lowest dose of TLO tested (0.9 nM TLO), and the percentage of cells perforated increased in a dose-dependent manner (**Fig. 4A**). These cells appeared to undergo membrane recovery by 30 min post-treatment, as dye uptake did not change from background for all TLO concentrations tested (Fig. 4B). Significant LDH release was not evident until exposure of BMDM to a much higher dose of 18.3 nM TLO (Fig. 4C). Thus, it appears that although cells become perforated starting at low levels of toxin, a high threshold of toxin must be reached before passive release of intracellular components occurs. IL-1β release in response to varying concentrations of TLO was then measured by ELISA (Fig. 4D). Maximal secretion of IL-1β occurred at 9.1 nM, a concentration that resulted in <10% LDH release. Strikingly, high levels of TLO, which resulted in correspondingly higher LDH release, induced lower levels of IL-1β secretion.

We next determined whether IL-1β released from cells was processed to the mature bioactive form by analyzing supernatants using Western blotting. A majority of the IL-1β was fully processed in supernatants from cells treated with 1.8 nM TLO,

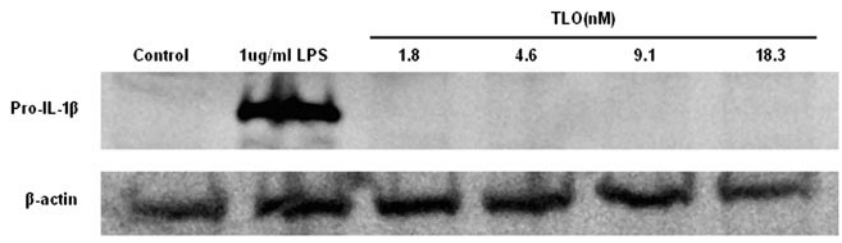

Figure 1. TLO cannot replace LPS as signal 1. BMDM were treated with control (DTT-containing buffer), 1 μg/ml LPS, 1.8 nM TLO (100 ng/ml TLO), 4.6 nM TLO (250 ng/ml TLO), 9.1 nM TLO (500 ng/ml TLO), or 18.3 nM TLO (1 μg/ml TLO) for 4 h in serum-containing media. Lysates were prepared from these cells, 50 μg protein run on a SDS-PAGE gel, and Western blot conducted for IL-1β protein. Only LPS treatment induces the detectable expression of 35 kDa pro-IL-1β. Data shown are a representative example of two independent experiments.

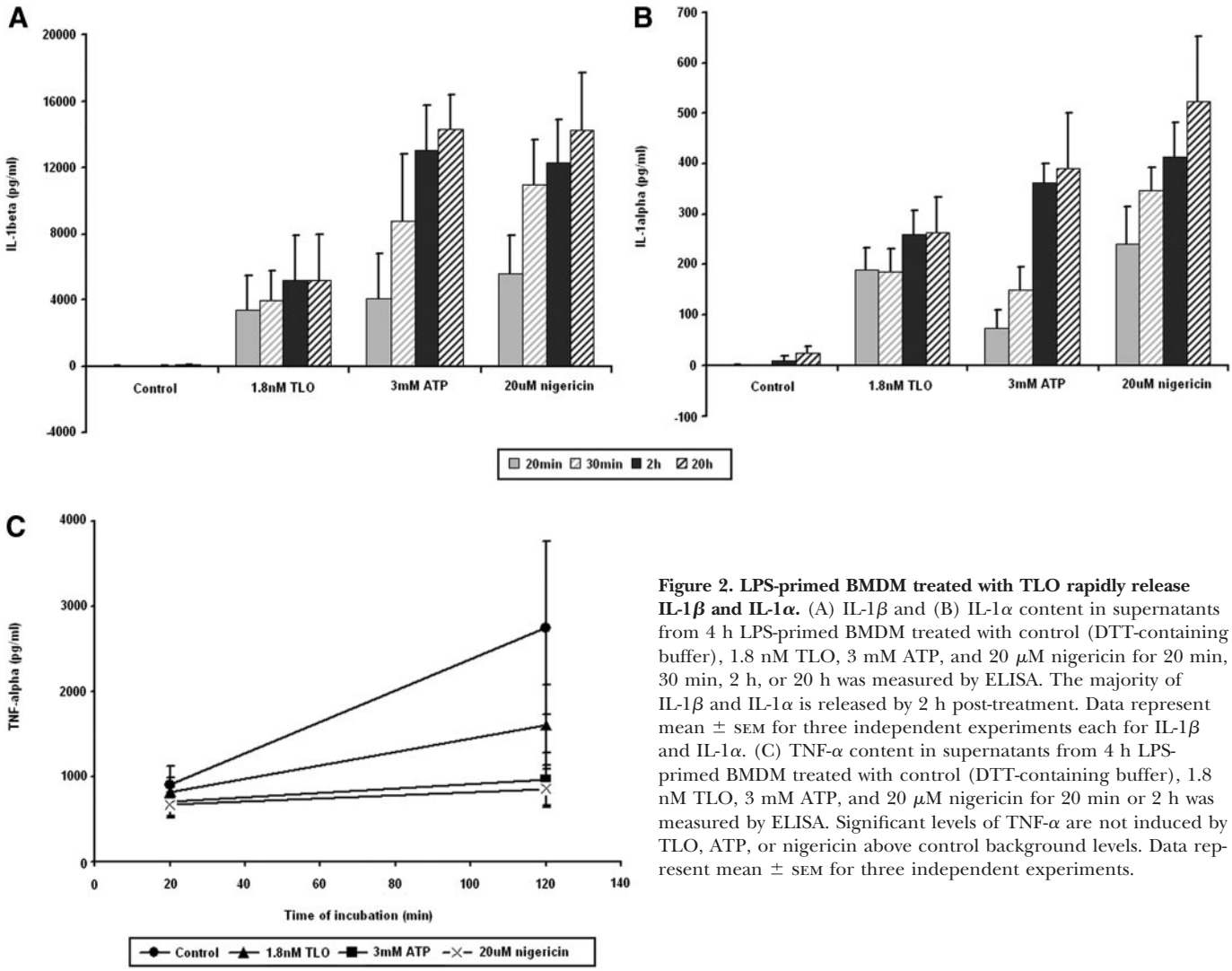

Figure 2. LPS-primed BMDM treated with TLO rapidly release IL-1β and IL-1α. (A) IL-1β and (B) IL-1α content in supernatants from 4 h LPS-primed BMDM treated with control (DTT-containing buffer), 1.8 nM TLO, 3 mM ATP, and 20 μM nigericin for 20 min, 30 min, 2 h, or 20 h was measured by ELISA. The majority of IL-1β and IL-1α is released by 2 h post-treatment. Data represent mean ± SEM for three independent experiments each for IL-1β and IL-1α. (C) TNF-α content in supernatants from 4 h LPS-primed BMDM treated with control (DTT-containing buffer), 1.8 nM TLO, 3 mM ATP, and 20 μM nigericin for 20 min or 2 h was measured by ELISA. Significant levels of TNF-α are not induced by TLO, ATP, or nigericin above control background levels. Data represent mean ± SEM for three independent experiments.

whereas in supernatants from cells treated with 9.1 nM or 18.3 nM TLO, much of the IL-1β was in the pro-form, and a less-mature form was detected (**Fig. 5A**). We also confirmed that 3 mM ATP and 20 μM nigericin induced the release of mostly mature IL-1β and 1% Triton X-100 lysed cells for complete release of pro-IL-1β content. As caspase-1 is known to cleave pro-IL-1β to its mature form and undergo cleavage and release itself after activation, we further tested for release of the p20 caspase-1 cleavage product after exposure to TLO. Mature p20 caspase-1 release only occurred at the low 1.8-nM TLO dose, and pro-caspase-1 was released from cells treated with high 9.1 nM or 18.3 nM TLO doses (Fig. 5B). ATP and nigericin controls also induced caspase-1 cleavage, but mature caspase-1 stayed inside the cells after ATP treatment, and nigericin treatment induced most of it to be secreted from the cells. Triton X-100 caused complete lysis and release of pro-caspase-1 stores. We found the same pattern of IL-1β content in these samples as shown in Figure 4D (data not shown). Thus, cleavage of pro-caspase-1 for release of mature caspase-1 and secretion of mature bioactive IL-1β by BMDM occur selectively at concentrations of toxin that are essentially nonlytic.

IL-1β induced by low doses of TLO requires potassium efflux, calcium influx, and the activities of calcium-independent PLA_2, caspase-1, and cathepsin B

To further elucidate the mechanism of IL-1β secretion induced by sublytic doses of TLO, we used a pharmacologic approach to inhibit different processes known to play a role in IL-1β secretion induced by other stimuli. Potassium efflux from cells, shown to be important for ATP and nigericin-induced IL-1β release, can be inhibited by addition of excess exogenous KCl to the medium. **Figure 6A** demonstrates that KCl also inhibited IL-1β release induced by TLO. It has also been shown that IL-1β secretion induced by ATP requires calcium influx. Treatment of BMDM with intracellular calcium chelator BAPTA-AM (Fig. 6B) prior to TLO exposure blocked IL-1β secretion similarly to that for ATP and nigericin. Another event that occurs during ATP-induced IL-1β release is

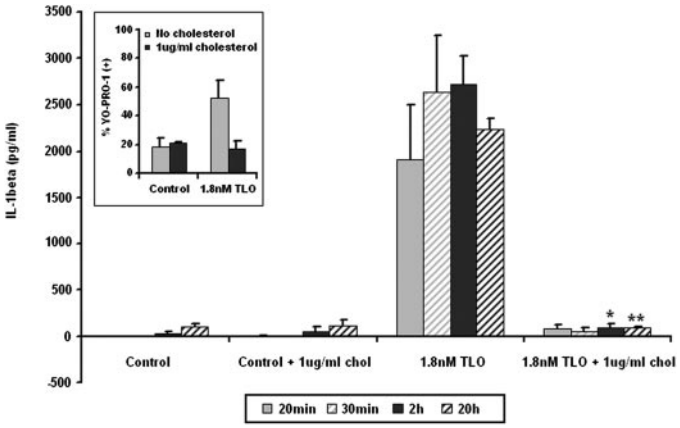

Figure 3. TLO-induced pore formation is required for IL-1β release from BMDM. Four-hour LPS-primed BMDM were treated with control (DTT-containing buffer), control plus 1 μg/ml cholesterol, 1.8 nM TLO, or 1.8 nM TLO plus 1 μg/ml cholesterol for 20 min, 30 min, 2 h, or 20 h. Supernatants were collected and assayed by ELISA for IL-1β. Free cholesterol inhibits TLO-induced IL-1β release. Data represent mean ± SEM for three independent experiments. Student's paired *t*-test was applied for comparison of the 1.8-nM TLO group with cholesterol versus without cholesterol; *, $P \leq 0.05$; **, $P \leq 0.01$. (Inset) Four-hour LPS-primed BMDM were treated with DTT control buffer or 1.8 nM TLO in the presence or absence of 1 μg/ml cholesterol for 5 min. TLO-induced perforation as measured by YO-PRO-1 dye uptake was assessed by flow cytometry. Free cholesterol blocks TLO from forming pores and allowing dye uptake. Data represent mean ± SEM for two independent experiments.

the activation of $iPLA_2$, which is also involved in TLO-induced IL-1β secretion, as tested by the $iPLA_2$ inhibitor BEL (Fig. 6C). Lastly, ion fluxes and $iPLA_2$ activity are thought to be involved in the activation of caspase-1, which in turn, cleaves pro-IL-1β to the mature form before its release. Pan-caspase inhibitor z-VAD-fmk and caspase-1-specific inhibitor Ac-YVAD-cmk each inhibited TLO-induced IL-1β secretion (Fig. 6D). Similar inhibition was seen with ATP and nigericin controls. All of the above pharmacological inhibitors were tested for toxicity against BMDM using YO-PRO-1 dye uptake (data not shown). It was found that BMDM exposed to 50 mM KCl, 30 μM BAPTA-AM, 10 μM BEL, 20 μM z-VAD-fmk, 100 μM Ac-YVAD-cmk, 100 μM pepstatin A, 100 μM CA-074-Me, or 10 μM Z-FF-fmk for 1 h did not take up YO-PRO-1 above background levels observed for untreated BMDM. Thus, the inhibitors used at these concentrations were not toxic to BMDM. Overall, these results demonstrate that sublytic TLO doses induce IL-1β secretion through similar mechanisms of that for ATP and nigericin.

It was reported recently that IL-1β released from cells exposed to silica and alum crystals, and also amyloid-β fibrils, required cathepsin B activity [35, 37]. Both groups proposed the novel hypothesis that cathepsin B localization to the cytosol might participate in IL-1β processing. We therefore investigated the role of cathepsin B activity in toxin-induced IL-1β release by using the highly selective cathepsin B inhibitor CA-074-Me. IL-1β release induced by a low dose of TLO was blocked substantially by this inhibitor (Fig. 6E). We also tested the contribution of other cathepsins in IL-1β release by using specific inhibitors pepstatin A (Fig. 6E) and Z-FF-fmk (Fig. 6F) to inhibit cathepsin D and cathepsin L activities, respectively. Little if any effect on TLO-induced IL-1β was observed with these inhibitors, suggesting that cathepsin D and L do not participate in toxin-induced cytokine release. ATP and nigericin showed a similar dependence on cathepsin B, with a partial contribution of cathepsin L evident for both of these stimuli. These results demonstrate that cathepsin B activity is required for release of IL-1β induced by sublytic TLO doses.

TLO-induced mature IL-1β release is dependent on the NLRP3 inflammasome

As ion fluxes, $iPLA_2$, caspase-1, and the release of IL-1β have all been linked to inflammasome activation, specifically, the NLRP3 inflammasome, we sought to determine if NLRP3 played a role in TLO-induced IL-1β secretion. To test this, we compared the response of wild-type, NLRP3-deficient, and NLRC4-deficient BMDM to a low dose of TLO (1.8 nM). We observed that 1.8 nM TLO induced mature IL-1β release from LPS-primed wild-type BMDM as well as $NLRC4^{-/-}$ BMDM but not $NLRP3^{-/-}$ BMDM (**Fig. 7A**). Similar results were obtained with the nigericin control, and Triton X-100 lysis caused release of pro-IL-1β, regardless of a NLRC4 or NLRP3 deficiency. Furthermore, a high dose of TLO (18.3 nM) induced release of the pro form from wild-type and $NLRP3^{-/-}$ BMDM (Fig. 7B). Taken together, these results demonstrate NLRP3 dependence for mature IL-1β release caused by a low dose of TLO but NLRP3 independence for pro-IL-1β secretion after exposure to a high TLO dose.

Toxin-induced pore formation is necessary but not sufficient for IL-1β release

We hypothesized, based on the above results, that pore formation would not be sufficient to induce IL-1β release by TLO in the absence of other components of the signaling pathway we identified. First, we assessed the ability of toxin to bind BMDM in the presence and absence of cholesterol using live cell confocal imaging to characterize the interaction. Cy5-labeled TLO was generated for this purpose, and BMDM were labeled with LysoTracker™ Green as a marker of internal compartments. Active TLO-Cy5 (noncholesterol-treated) bound predominantly to the surface of BMDM (**Fig. 8A**). On the other hand, BMDM internalized cholesterol-bound TLO-Cy5 to mostly nonacidic compartments, as there was little colocalization observed with LysoTracker™ Green-labeled vesicles (Fig. 8B). To next test if binding and pore formation could occur in the presence of inhibitors of IL-1β release, the interaction between Cy5-labeled TLO and BMDM was measured by flow cytometry. Pore formation was measured by uptake of YO-PRO-1 dye. Fluorescently labeled TLO binds to cells and perforates them, as evidenced by increased YO-PRO-1 uptake (Fig. 8C) and increased Cy5 signal (Fig. 8D), relative to cells exposed to labeled BSA used as a control. In the presence of BAPTA-AM or KCl, which impairs IL-1β secretion as discussed previously, binding of TLO and subsequent pore formation are essentially unaffected. It can again be seen that Cy5-

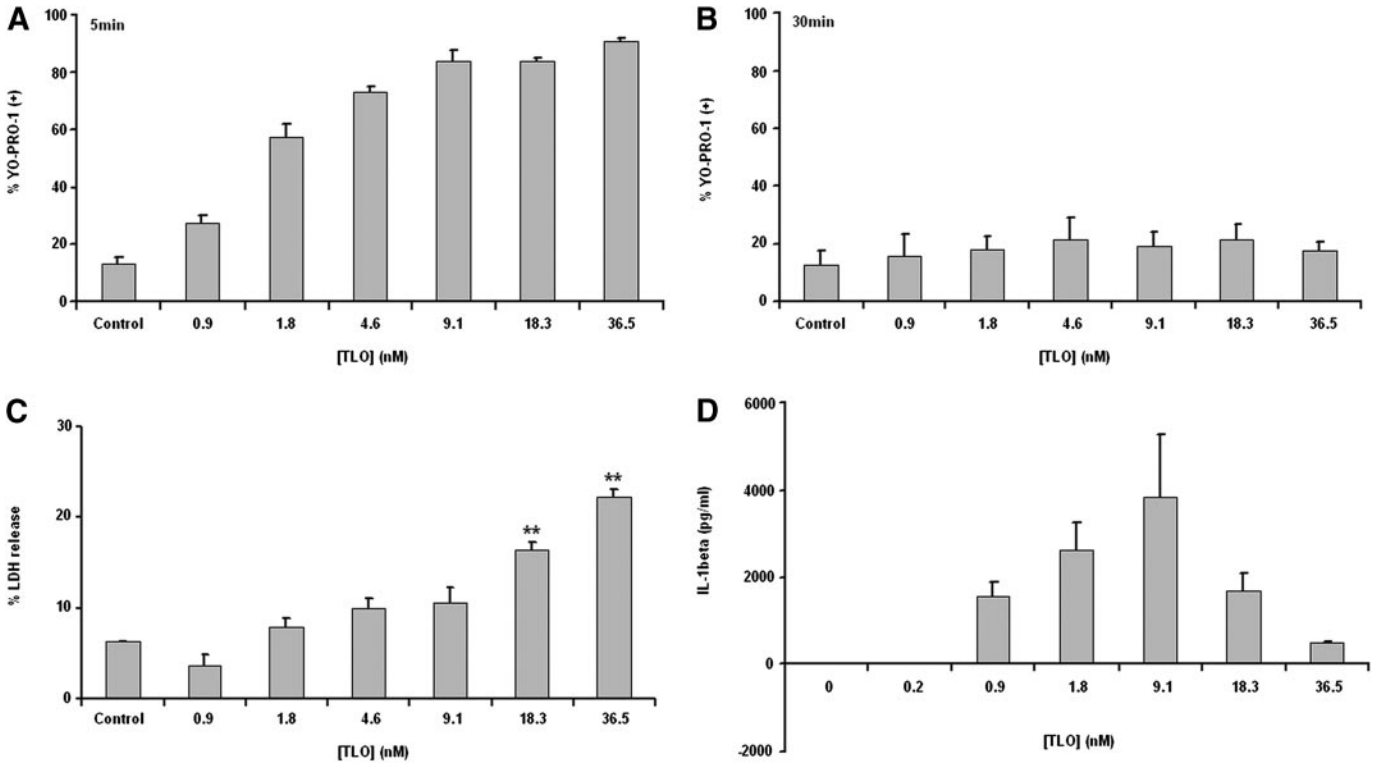

Figure 4. Determination of sublytic versus lytic CDC doses. (A and B) Four-hour LPS-primed BMDM were treated with DTT control buffer or a range of TLO doses in serum-free media for 5 min or 30 min. BMDM were harvested and stained with YO-PRO-1 dye as a measure of TLO-induced perforation, and dye uptake was assessed by flow cytometry. BMDM are perforated after 5 min of exposure to 0.9 nM TLO, and this process occurs in a dose-dependent manner. By 30 min post-TLO treatment, BMDM are no longer perforated. Data represent mean ± SEM for three independent experiments for each time-point. (C) Supernatants were collected from 4 h LPS-primed BMDM treated for 30 min with DTT control buffer or various TLO doses in serum-free media. TLO-induced passive spilling of contents (i.e., LDH) was determined by taking the ratio of LDH released from TLO-treated BMDM to LDH released from Triton X-100-treated BMDM (see Materials and Methods). In comparison with perforation at lower doses of TLO, BMDM do not release LDH until much higher doses (18.3 nM) of TLO. Data represent mean ± SEM for three independent experiments. Student's paired *t*-test was applied for comparison of control versus TLO conditions; **, $P \leq 0.01$. (D) Four-hour LPS-primed BMDM were treated with a range of concentrations of TLO for 30 min. Supernatants were collected and assayed by ELISA for IL-1β. Release of IL-1β from BMDM occurs after treatment with 0.9–36.5 nM TLO. Data represent mean ± SEM for three independent experiments.

labeled TLO preincubated with cholesterol associates with BMDM, despite the lack of pore-forming activity. Taken together with the microscopy data, these results show that cholesterol-bound TLO can be internalized efficiently by BMDM without causing deleterious effects and without inducing biological responses such as IL-1β secretion. Overall, these results demonstrate that TLO-induced pore formation is required but not sufficient for IL-1β release from BMDM.

DISCUSSION

We show here that TLO, a toxin of the CDC family, induces the rapid release of IL-1β from LPS-primed murine BMDM. Release of this cytokine typically requires two stimuli: TLR pathway activation to generate the inactive IL-1β precursor and a stimulator of the inflammasome for the activation of caspase-1 to cleave pro-IL-1β to its mature form before release. It has been observed that signal 1 (e.g., LPS) alone or signal 2 (e.g., ATP) alone stimulates IL-1β release from macrophages at low levels (pg/ml range for in vitro cultures), usually over long time periods (up to 24 h) [47, 49]. However, when both signals are applied sequentially, IL-1β can be secreted from macrophages in large amounts (ng/ml range) within 30 min [28, 50]. Our results are consistent with TLO acting as a type of signal 2 and are inconsistent with TLO providing signal 1 to BMDM.

Shoma et al. [47] reported recently that the CDC PLY induced the release of IL-1β and IL-1α from murine peritoneal macrophages, a TLR4-dependent process not inhibited by cholesterol [47]. The PLY doses used in those experiments were similar to those for TLO used in our experiments. Additionally, other groups have found that PLY induces IL-1β secretion from monocytes [20] and that CDC LLO induces IL-1 (type not defined) release from peritoneal macrophages [51], a process also unaffected by free cholesterol. In contrast, we tested whether TLO could induce release of IL-1β from LPS-primed BMDM, which carry pre-formed stores of the cytokine. Our results demonstrate that TLO-induced pore formation, requiring binding of the toxin to cellular cholesterol, stimulates the

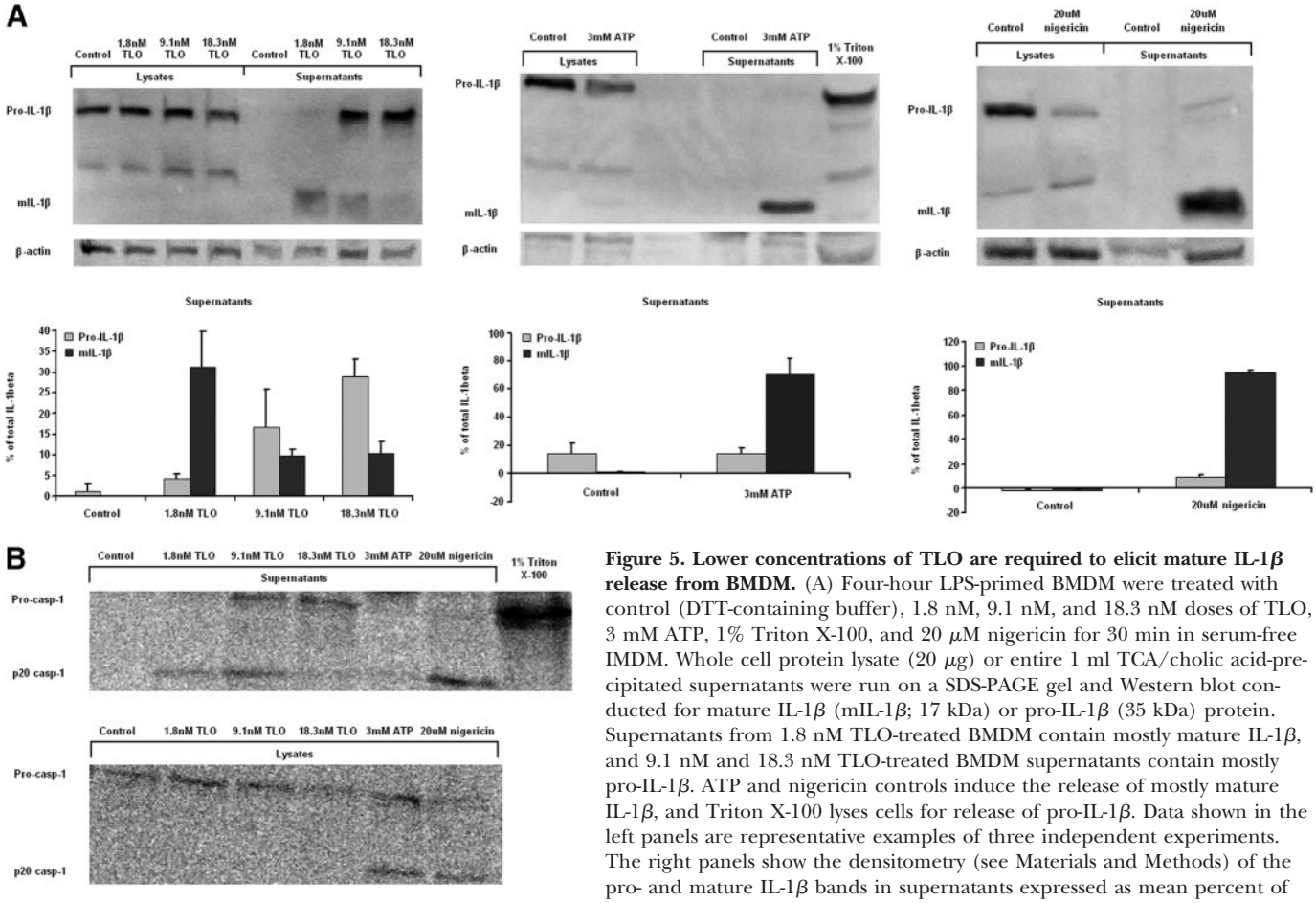

Figure 5. Lower concentrations of TLO are required to elicit mature IL-1β release from BMDM. (A) Four-hour LPS-primed BMDM were treated with control (DTT-containing buffer), 1.8 nM, 9.1 nM, and 18.3 nM doses of TLO, 3 mM ATP, 1% Triton X-100, and 20 μM nigericin for 30 min in serum-free IMDM. Whole cell protein lysate (20 μg) or entire 1 ml TCA/cholic acid-precipitated supernatants were run on a SDS-PAGE gel and Western blot conducted for mature IL-1β (mIL-1β; 17 kDa) or pro-IL-1β (35 kDa) protein. Supernatants from 1.8 nM TLO-treated BMDM contain mostly mature IL-1β, and 9.1 nM and 18.3 nM TLO-treated BMDM supernatants contain mostly pro-IL-1β. ATP and nigericin controls induce the release of mostly mature IL-1β, and Triton X-100 lyses cells for release of pro-IL-1β. Data shown in the left panels are representative examples of three independent experiments. The right panels show the densitometry (see Materials and Methods) of the pro- and mature IL-1β bands in supernatants expressed as mean percent of total IL-1β in supernatants ± SEM for three independent experiments. (B) BMDM were treated as in part A. Whole cell protein lysate (20 μg) or entire 1 ml TCA/cholic acid-precipitated supernatant was run on a SDS-PAGE gel and Western blot conducted for pro-caspase-1 (45 kDa) or the cleaved p20 caspase-1 subunit (20 kDa). Supernatants from 1.8 nM TLO-treated BMDM contain mostly p20 caspase-1, and 9.1 nM and 18.3 nM TLO-treated BMDM supernatants contain pro-caspase-1. ATP and nigericin controls induce the cleavage of pro-caspase-1 with release of the p20 subunit from nigericin-treated cells and retained p20 for ATP-treated cells. Triton X-100 lyses cells for release of pro-caspase-1. Data shown are a representative example of two independent experiments.

rapid release of large amounts of cytokine through a mechanism dependent on K^+ efflux, Ca^{2+} influx, and the activation of iPLA2, NLRP3, caspase-1, and cathepsin B. It should be noted that there was some variation in the amounts of TLO-induced IL-1β (mean amount/experiment ranged from 1975 to 3973 pg/ml; minimum=803 pg/ml; maximum=7569 pg/ml). The spread in values is most likely a result of several factors, such as differences in macrophage batch preparation, macrophage harvest day (as BMDM were maintained in culture up to 3 weeks), sample collection day, and assay day.

It appears that TLO-induced pore formation causes K^+ efflux and subsequent IL-1β release. However, mature IL-1β release only occurs when pore formation is balanced by the ability of cells to maintain function, required presumably for the activation of appropriate signaling pathways that will lead to the activation of caspase-1, the protease responsible for the conversion of inactive pro-IL-1β to active, mature IL-1β. Evidence for this is seen at low concentrations of TLO, which induced release of primarily mature IL-1β as well as cleaved, mature caspase-1, whereas higher doses caused release of the pro-forms of caspase-1 and IL-1β predominantly, which are biologically inactive. We suggest that at high concentrations of toxin, a cell may undergo rapid release of contents (e.g., pro-caspase-1 and pre-formed pro-IL-1β stores) through a passive process, outpacing the ability of the cell to activate caspase-1, required for processing of the pro- to mature form. This finding may explain a difference between our results and those of Kanneganti et al. [31], who reported that CDC SLO does not activate caspase-1. In their study, SLO was used at a high dose of 5 μg/ml or 72.5 nM.

In addition to a requirement for K^+ efflux, we identified calcium influx and the activities of $iPLA_2$, NLRP3, and caspase-1 as key players in TLO-induced IL-1β release. To our knowledge, this is the first study to address the mechanism of CDC-induced IL-1β release and to differentiate the effects of low versus high toxin doses. Noncholesterol binding, PFTs from other families, such as *Aeromonas hydrophila* aerolysin, which binds to GPI-anchored protein receptors, and Staphylococcus *aureus* α-toxin, which binds specific lipid clusters [52], have also been shown to require K+ efflux for their down-

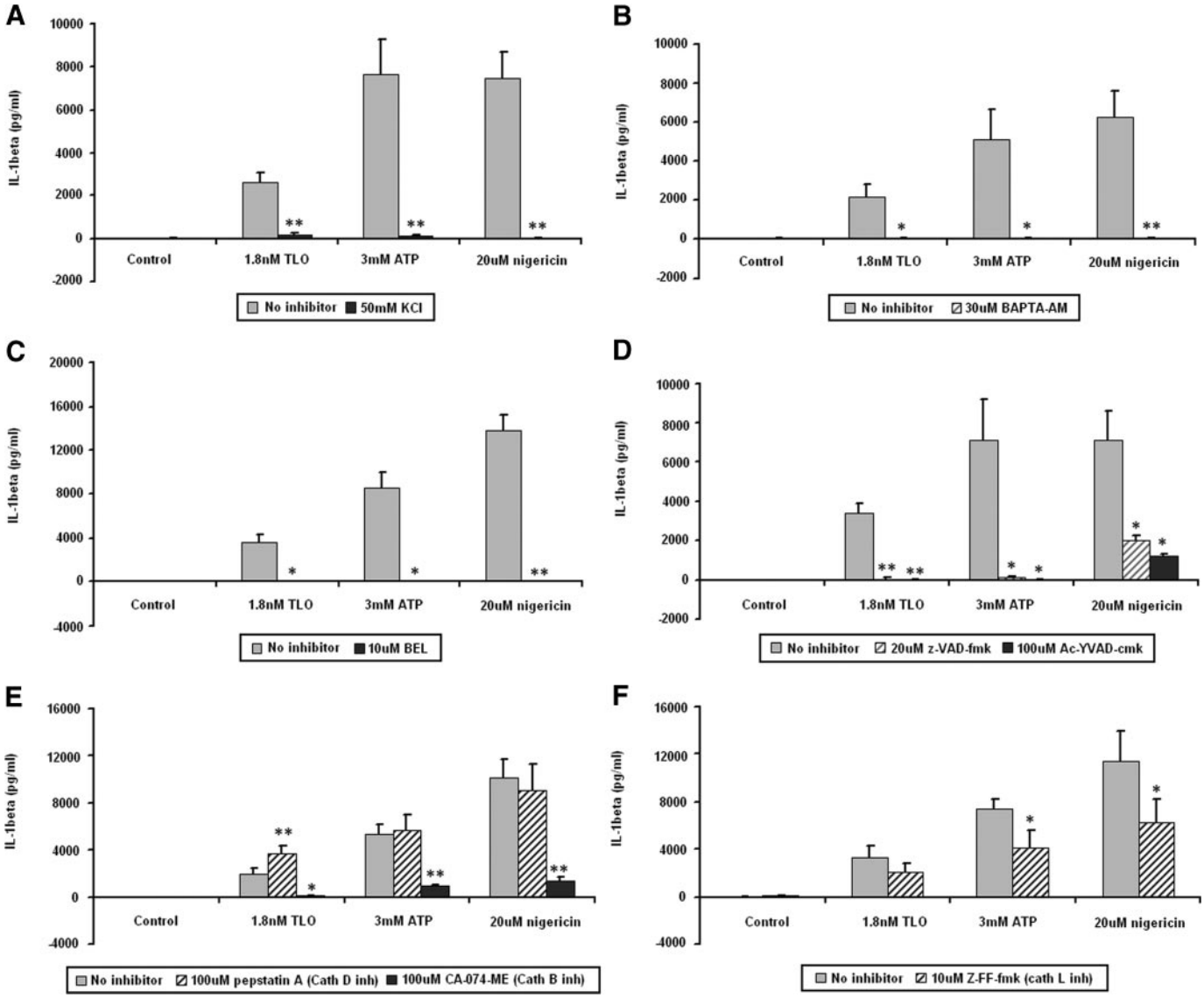

Figure 6. TLO-induced IL-1β release from BMDM relies on K^+ efflux, Ca^{2+} influx, and the activities of $iPLA_2$, caspase-1, and cathepsin B. Four-hour LPS-primed BMDM were treated with no inhibitor (buffer only) versus 50 mM KCl (K^+ efflux inhibitor; A), 30 μM BAPTA-AM (intracellular calcium chelator; B), 10 μM BEL ($iPLA_2$ inhibitor; C), 20 μM z-VAD-fmk (pan-caspase inhibitor) or 100 μM Ac-YVAD-cmk (caspase-1 inhibitor; D), 100 μM pepstatin A (cathepsin D inhibitor) or 100 μM CA-074-Me (cathepsin B inhibitor; E), or 10 μM Z-FF-fmk (cathepsin L inhibitor; F) for 1 h. Control (DTT-containing buffer), 1.8 nM TLO, 3 mM ATP, or 20 μM nigericin treatments were then added for 30 min. Supernatants were collected and assayed by ELISA for IL-1β. KCl, BAPTA-AM, BEL, z-VAD-fmk, and Ac-YVAD-cmk almost completely abrogate IL-1β secretion induced by TLO, ATP, and nigericin. Cathepsin B inhibitor CA-074-Me has a major effect on IL-1β secretion induced by all three stimuli, and the other cathepsins play a lesser role. It should be noted that all inhibitors were not toxic to cells, as assessed by YO-PRO-1 dye uptake (data not shown). Data represent mean ± SEM for (A, D, and E) five independent experiments, (B) six independent experiments, (C) three independent experiments, and (F) four independent experiments. Student's paired *t*-test was applied for comparison of no inhibitor versus inhibitor conditions; *, $P \leq 0.05$; **, $P \leq 0.01$.

stream effects [53–55]. Aerolysin has been implicated in the activation of the NLRP3 and NLRC4 inflammasomes as well as caspase-1 for the activation of sterol regulatory element-binding proteins, which promote cell survival after cell membrane injury [53]. However, this study used nonimmune cells, and the role of aerolysin in IL-1β processing and release was not addressed. α-Toxin has also been shown to induce IL-1β secretion from LPS-primed monocytes, but the mechanism of release is unclear [55, 56]. It should be stressed that although these other toxins may share some similarities to CDC in their ability to form pores in cells and initiate K+ efflux, they also differ in pore size (2 nm for aerolysin and α-toxin; 30 nm for CDC) [52] and therefore, could have divergent downstream pathways. One such example is the response of cells to α-toxin-mediated versus CDC-mediated cell injury. It has been observed that membrane repair after CDC-induced injury involves a p38-independent mechanism and occurs in less than 1 h compared with α-toxin-

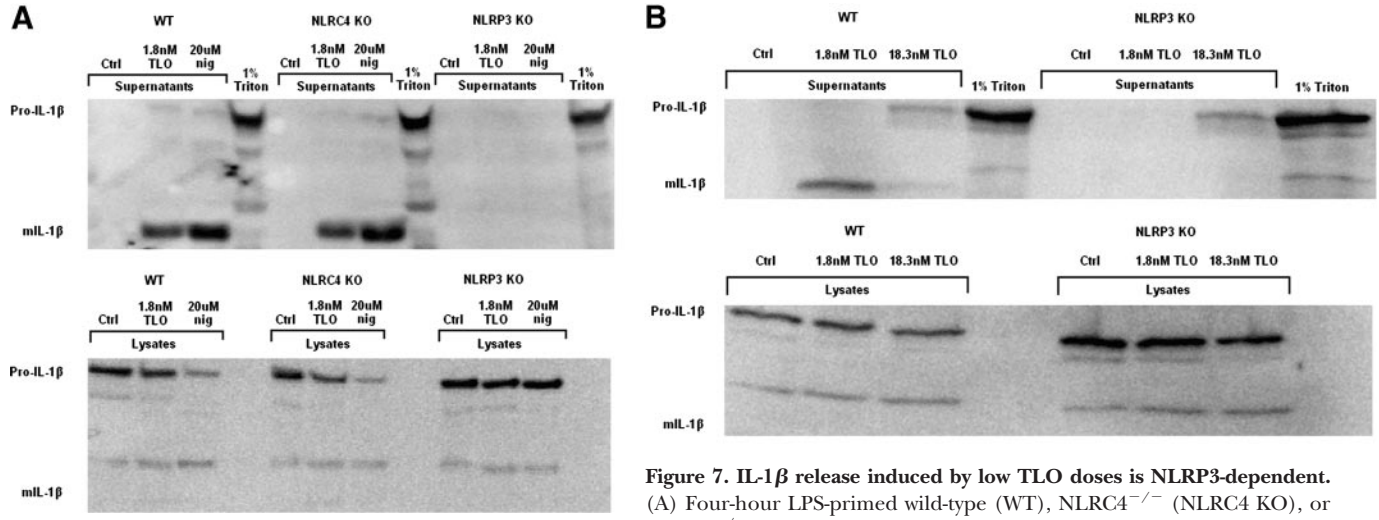

Figure 7. IL-1β release induced by low TLO doses is NLRP3-dependent. (A) Four-hour LPS-primed wild-type (WT), NLRC4$^{-/-}$ (NLRC4 KO), or NLRP3$^{-/-}$ (NLRP3 KO) BMDM were treated with control (DTT-containing buffer), 1.8 nM TLO, 20 uM nigericin, or 1% Triton X-100 for 30 min in serum-free IMDM. Whole cell protein lysate (20 μg) or entire 1 ml TCA/cholic acid-precipitated supernatants were run on a SDS-PAGE gel and Western blot conducted for mature (17 kDa) or pro (35 kDa)-IL-1β protein. Mature IL-1β was released from wild-type and NLRC4$^{-/-}$ BMDM after exposure to the low TLO dose and nigericin but not from NLRP3$^{-/-}$ BMDM. Triton X-100 lysis caused release of pro-IL-1β stores from all cell types, including NLRP3$^{-/-}$ BMDM. Data shown are representative examples of two independent experiments. (B) Four-hour LPS-primed wild-type or NLRP3$^{-/-}$ BMDM were treated with control (DTT-containing buffer), 1.8 nM TLO (low dose), 18.3 nM TLO (high dose), or 1% Triton X-100 for 30 min in serum-free IMDM. Whole cell protein lysate (20 μg) or entire 1 ml TCA/cholic acid-precipitated supernatants were run on a SDS-PAGE gel and Western blot conducted for mature (17 kDa) or pro (35 kDa)-IL-1β protein. Mature IL-1β was released from wild-type BMDM after exposure to the low TLO dose but not from NLRP3$^{-/-}$ BMDM. The high TLO dose as well as Triton X-100 caused release of pro-IL-1β stores from wild-type and NLRP3$^{-/-}$ BMDM. Data shown are a representative example of three independent experiments.

mediated repair that requires p38 activity and may take many hours for full recovery [14, 57]. Thus, it will be interesting to see if IL-1β processing and release mechanisms are similar or disparate for PFTs that form small pores (α-toxin, aerolysin) versus large ones (CDC).

Although the involvement of ion fluxes and the activities of iPLA$_2$, NLRP3, and caspase-1 in IL-1β release induced by ATP and nigericin are well established [58], the mechanism for direct activation of the NLRP3 inflammasome complexes has remained unclear. Recently, studies by Hornung et al. [35] and Halle et al. [37] have suggested that cathepsin B may activate the NLRP3 inflammasome directly or indirectly through other factors. In their studies, they show that IL-1β-inducing stimuli, such as silica crystals, alum salt crystals, and amyloid-β fibrils, are phagocytosed and that these cargos disrupt lysosomal integrity. This would allow subsequent release of cathepsin B into the cytosol, which is proposed to cause activation of the NLRP3 inflammasome by an unknown mechanism. We also observe a dependence on cathepsin B activity for TLO-induced IL-1β secretion. Studies are under way to determine if this toxin relies on similar pathways as silica crystals, alum salt crystals, and amyloid-β fibrils, which lead to active cytosolic cathepsin B.

In addition to understanding how caspase-1 is activated directly in this system, there is much interest in determining the general mechanism by which mature IL-1β is secreted from cells. IL-1β lacks signal sequences for localization to the Golgi and other classical secretory compartments and therefore, must be secreted by nonclassical means. The data available suggest several possible, different pathways, including release of exosomes carrying mature IL-1β after fusion of multivesicular bodies with the plasma membrane, Ca^{2+}-dependent secretory lysosome exocytosis, microvesicle shedding from the plasma membrane, and direct translocation of cytosolic cytokine through unknown plasma membrane transporters to the extracellular environment [42]. It is possible that multiple pathways may be involved for a single cell type or that a particular pathway is designated to each specific cell type. At this time, it is unknown what pathway(s) TLO uses to export mature IL-1β.

This is the first study to identify the mechanism of IL-1β release induced by a family of cholesterol-binding, large PFTs and to distinguish the IL-1β response to lower versus higher toxin doses. This IL-1β release mechanism may differ from that for other families of PFTs that bind different receptors, form much smaller pores, and use different pathways to achieve the same goal (i.e., pore-resealing processes). Moreover, to our knowledge, this is the first observation of cathepsin B involvement in IL-1β release induced by a PFT. In summary, we find that low TLO concentrations induce the rapid release of relatively high amounts of active, mature IL-1β from LPS-primed murine macrophages in a process dependent on toxin-induced perforation, potassium efflux, calcium influx, and activation of iPLA$_2$, NLRP3, caspase-1, and cathepsin B. On the other hand, high TLO doses induce the release of inactive pro-IL-1β, which may be an evasion mechanism used by bacteria during infection. This study addresses in detail the mechanisms of CDC-induced, rapid IL-1β release and may

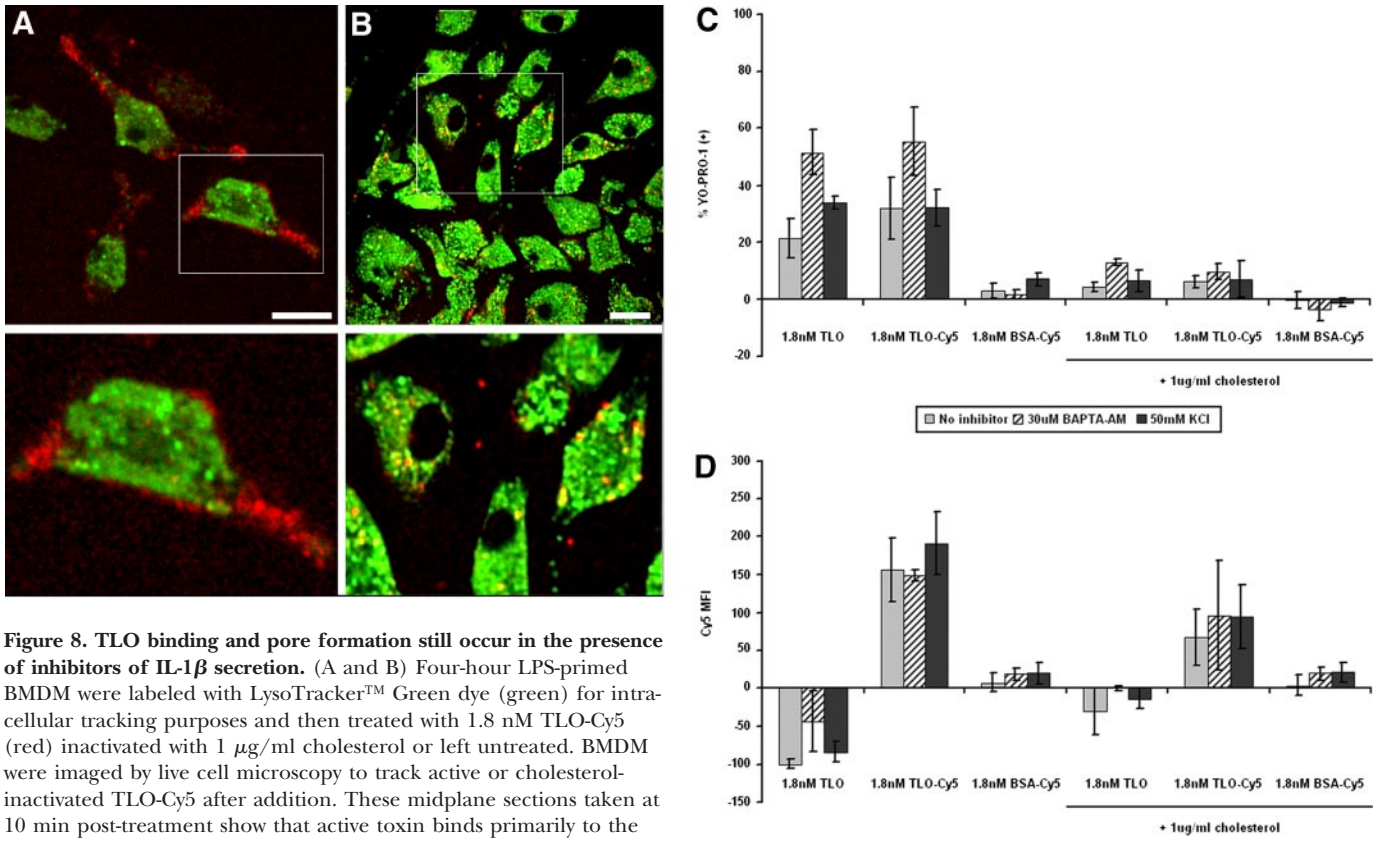

Figure 8. TLO binding and pore formation still occur in the presence of inhibitors of IL-1β secretion. (A and B) Four-hour LPS-primed BMDM were labeled with LysoTracker™ Green dye (green) for intracellular tracking purposes and then treated with 1.8 nM TLO-Cy5 (red) inactivated with 1 μg/ml cholesterol or left untreated. BMDM were imaged by live cell microscopy to track active or cholesterol-inactivated TLO-Cy5 after addition. These midplane sections taken at 10 min post-treatment show that active toxin binds primarily to the surface of BMDM (A), and cholesterol-bound toxin is internalized by BMDM (B). The lower panels show magnifications of boxed cells displayed in the upper panels. Original white bar scales indicate a 10-μm length. (C and D) Four-hour LPS-primed BMDM were treated with no inhibitor (buffer only), 50 mM KCl, or 30 μM BAPTA-AM for 1 h, followed by addition of control (DTT-containing buffer), 1.8 nM TLO, 1.8 nM TLO-Cy5, or 1.8 nM BSA-Cy5 in the presence or absence of 1 μg/ml cholesterol for 5 min. BMDM were analyzed by flow cytometry for TLO-induced pore formation (YO-PRO-1 uptake; A) and TLO binding (Cy5 signal; B). BMDM bind to pore-inducing TLO-Cy5, but not control BSA-Cy5, in the absence of IL-1β inhibitors as well as in the presence of BAPTA-AM or KCl. Data represent mean ± SEM for three independent experiments. Control background values were subtracted out from the data. MFI, Mean fluorescence intensity.

help to explain the effects of these toxins in bacterial infections and the subsequent host immune responses.

ACKNOWLEDGMENTS

This work was supported by National Institutes of Health grants AI57168 (R. D. S. and S. C. W.), CA73743 (R. D. S.), CA082084 (J. C. and L. M. T.), AI063331 (L. F. and G. N.), and AI064748 (L. F. and G. N.). We are grateful to Dr. Lisa Borghesi for providing wild-type mouse bone marrow. We also appreciate the technical help from and useful personal communications with Dr. Chengqun Sun and Michelle Heid and technical support from Sarita Singh.

REFERENCES

1. Billington, S. J., Jost, B. H., Songer, J. G. (2000) Thiol-activated cytolysins: structure, function and role in pathogenesis. *FEMS Microbiol. Lett.* **182,** 197–205.
2. Palmer, M. (2001) The family of thiol-activated, cholesterol-binding cytolysins. *Toxicon* **39,** 1681–1689.
3. Bhakdi, S., Tranum-Jensen, J., Sziegoleit, A. (1985) Mechanism of membrane damage by streptolysin-O. *Infect. Immun.* **47,** 52–60.
4. Morgan, P. J., Hyman, S. C., Rowe, A. J., Mitchell, T. J., Andrew, P. W., Saibil, H. R. (1995) Subunit organization and symmetry of pore-forming, oligomeric pneumolysin. *FEBS Lett.* **371,** 77–80.
5. Olofsson, A., Hebert, H., Thelestam, M. (1993) The projection structure of perfringolysin O (Clostridium perfringens θ-toxin). *FEBS Lett.* **319,** 125–127.
6. Watanabe, I., Nomura, T., Tominaga, T., Yamamoto, K., Kohda, C., Kawamura, I., Mitsuyama, M. (2006) Dependence of the lethal effect of pore-forming haemolysins of Gram-positive bacteria on cytolytic activity. *J. Med. Microbiol.* **55,** 505–510.
7. Benton, K. A., Everson, M. P., Briles, D. E. (1995) A pneumolysin-negative mutant of *Streptococcus pneumoniae* causes chronic bacteremia rather than acute sepsis in mice. *Infect. Immun.* **63,** 448–455.
8. Berry, A. M., Yother, J., Briles, D. E., Hansman, D., Paton, J. C. (1989) Reduced virulence of a defined pneumolysin-negative mutant of *Streptococcus pneumoniae. Infect. Immun.* **57,** 2037–2042.
9. Cowan, G. J., Atkins, H. S., Johnson, L. K., Titball, R. W., Mitchell, T. J. (2007) Immunization with anthrolysin O or a genetic toxoid protects against challenge with the toxin but not against *Bacillus anthracis. Vaccine* **25,** 7197–7205.
10. Beauregard, K. E., Lee, K. D., Collier, R. J., Swanson, J. A. (1997) pH-Dependent perforation of macrophage phagosomes by listeriolysin O from *Listeria monocytogenes. J. Exp. Med.* **186,** 1159–1163.
11. Geoffroy, C., Gaillard, J. L., Alouf, J. E., Berche, P. (1987) Purification, characterization, and toxicity of the sulfhydryl-activated hemolysin listeriolysin O from *Listeria monocytogenes. Infect. Immun.* **55,** 1641–1646.
12. Wei, Z., Schnupf, P., Poussin, M. A., Zenewicz, L. A., Shen, H., Goldfine, H. (2005) Characterization of *Listeria monocytogenes* expressing anthrolysin O and phosphatidylinositol-specific phospholipase C from *Bacillus anthracis. Infect. Immun.* **73,** 6639–6646.
13. Mosser, E. M., Rest, R. (2006) The *Bacillus anthracis* cholesterol-dependent cytolysin, anthrolysin O, kills human neutrophils, monocytes and macrophages. *BMC Microbiol.* **6,** 56.
14. Husmann, M., Dersch, K., Bobkiewicz, W., Beckmann, E., Veerachato, G., Bhakdi, S. (2006) Differential role of p38 mitogen activated protein ki-

nase for cellular recovery from attack by pore-forming *S. aureus* [α]-toxin or streptolysin O. *Biochem. Biophys. Res. Commun.* **344,** 1128–1134.
15. Walev, I., Hombach, M., Bobkiewicz, W., Fenske, D., Bhakdi, S., Husmann, M. (2001) Resealing of large transmembrane pores produced by streptolysin O in nucleated cells is accompanied by NF-κB activation and downstream events. *FASEB J.* **16,** 237–239.
16. Idone, V., Tam, C., Goss, J. W., Toomre, D., Pypaert, M., Andrews, N. W. (2008) Repair of injured plasma membrane by rapid Ca2+-dependent endocytosis. *J. Cell Biol.* **180,** 905–914.
17. Henderson, B., Wilson, M., Wren, B. (1997) Are bacterial exotoxins cytokine network regulators? *Trends Microbiol.* **5,** 454–458.
18. Nishibori, T., Xiong, H., Kawamura, I., Arakawa, M., Mitsuyama, M. (1996) Induction of cytokine gene expression by listeriolysin O and roles of macrophages and NK cells. *Infect. Immun.* **64,** 3188–3195.
19. Hackett, S. P., Stevens, D. L. (1992) Streptococcal toxic shock syndrome: synthesis of tumor necrosis factor and interleukin-1 by monocytes stimulated with pyrogenic exotoxin A and streptolysin O. *J. Infect. Dis.* **165,** 879–885.
20. Houldsworth, S., Andrew, P. W., Mitchell, T. J. (1994) Pneumolysin stimulates production of tumor necrosis factor α and interleukin-1 β by human mononuclear phagocytes. *Infect. Immun.* **62,** 1501–1503.
21. Arend, W. P., Palmer, G., Gabay, C. (2008) IL-1, IL-18, and IL-33 families of cytokines. *Immunol. Rev.* **223,** 20–38.
22. Franchi, L., Eigenbrod, T., Munoz-Planillo, R., Nunez, G. (2009) The inflammasome: a caspase-1-activation platform that regulates immune responses and disease pathogenesis. *Nat. Immunol.* **10,** 241–247.
23. Martinon, F., Mayor, A., Tschopp, J. (2009) The inflammasomes: guardians of the body. *Annu. Rev. Immunol.* **27,** 229–265.
24. Pedra, J. H., Cassel, S. L., Sutterwala, F. S. (2009) Sensing pathogens and danger signals by the inflammasome. *Curr. Opin. Immunol.* **21,** 10–16.
25. Ferrari, D., Pizzirani, C., Adinolfi, E., Lemoli, R. M., Curti, A., Idzko, M., Panther, E., Di Virgilio, F. (2006) The P2X7 receptor: a key player in IL-1 processing and release. *J. Immunol.* **176,** 3877–3883.
26. Brough, D., Le Feuvre, R. A., Wheeler, R. D., Solovyova, N., Hilfiker, S., Rothwell, N. J., Verkhratsky, A. (2003) Ca2+ stores and Ca2+ entry differentially contribute to the release of IL-1 β and IL-1 α from murine macrophages. *J. Immunol.* **170,** 3029–3036.
27. Andrei, C., Margiocco, P., Poggi, A., Lotti, L. V., Torrisi, M. R., Rubartelli, A. (2004) Phospholipases C and A2 control lysosome-mediated IL-1 β secretion: implications for inflammatory processes. *Proc. Natl. Acad. Sci. USA* **101,** 9745–9750.
28. Sutterwala, F. S., Ogura, Y., Szczepanik, M., Lara-Tejero, M., Lichtenberger, G. S., Grant, E. P., Bertin, J., Coyle, A. J., Galan, J. E., Askenase, P. W., Flavell, R. A. (2006) Critical role for NALP3/CIAS1/cryopyrin in innate and adaptive immunity through its regulation of caspase-1. *Immunity* **24,** 317–327.
29. Locovei, S., Scemes, E., Qiu, F., Spray, D. C., Dahl, G. (2007) Pannexin1 is part of the pore forming unit of the P2X7 receptor death complex. *FEBS Lett.* **581,** 483–488.
30. Pelegrin, P., Surprenant, A. (2006) Pannexin-1 mediates large pore formation and interleukin-1β release by the ATP-gated P2X7 receptor. *EMBO J.* **25,** 5071–5082.
31. Kanneganti, T-D., Lamkanfi, M., Kim, Y-G., Chen, G., Park, J-H., Franchi, L., Vandenabeele, P., Nunez, G. (2007) Pannexin-1-mediated recognition of bacterial molecules activates the cryopyrin inflammasome independent of Toll-like receptor signaling. *Immunity* **26,** 433–443.
32. Mariathasan, S., Weiss, D. S., Newton, K., McBride, J., O'Rourke, K., Roose-Girma, M., Lee, W. P., Weinrauch, Y., Monack, D. M., Dixit, V. M. (2006) Cryopyrin activates the inflammasome in response to toxins and ATP. *Nature* **440,** 228–232.
33. Le Feuvre, R. A., Brough, D., Iwakura, Y., Takeda, K., Rothwell, N. J. (2002) Priming of macrophages with lipopolysaccharide potentiates P2X7-mediated cell death via a caspase-1-dependent mechanism, independently of cytokine production. *J. Biol. Chem.* **277,** 3210–3218.
34. Martinon, F., Petrilli, V., Mayor, A., Tardivel, A., Tschopp, J. (2006) Gout-associated uric acid crystals activate the NALP3 inflammasome. *Nature* **440,** 237–241.
35. Hornung, V., Bauernfeind, F., Halle, A., Samstad, E. O., Kono, H., Rock, K. L., Fitzgerald, K. A., Latz, E. (2008) Silica crystals and aluminum salts activate the NALP3 inflammasome through phagosomal destabilization. *Nat. Immunol.* **9,** 847–856.
36. Dostert, C., Petrilli, V., Van Bruggen, R., Steele, C., Mossman, B. T., Tschopp, J. (2008) Innate immune activation through Nalp3 inflammasome sensing of asbestos and silica. *Science* **320,** 674–677.
37. Halle, A., Hornung, V., Petzold, G. C., Stewart, C. R., Monks, B. G., Reinheckel, T., Fitzgerald, K. A., Latz, E., Moore, K. J., Golenbock, D. T. (2008) The NALP3 inflammasome is involved in the innate immune response to amyloid-β. *Nat. Immunol.* **9,** 857–865.
38. Willingham, S. B., Ting, J. P. (2008) NLRs and the dangers of pollution and aging. *Nat. Immunol.* **9,** 831–833.
39. Schotte, P., Van Criekinge, W., Van de Craen, M., Van Loo, G., Desmedt, M., Grooten, J., Cornelissen, M., De Ridder, L., Vandekerckhove, J., Fiers, W., Vandenabeele, P., Beyaert, R. (1998) Cathepsin B-mediated activation of the proinflammatory caspase-11. *Biochem. Biophys. Res. Commun.* **251,** 379–387.
40. Wang, S., Miura, M., Jung, Y. K., Zhu, H., Li, E., Yuan, J. (1998) Murine caspase-11, an ICE-interacting protease, is essential for the activation of ICE. *Cell* **92,** 501–509.
41. Davies, J. Q., Gordon, S. (2005) Isolation and culture of murine macrophages. *Methods Mol. Biol.* **290,** 91–103.
42. Qu, Y., Franchi, L., Nunez, G., Dubyak, G. R. (2007) Nonclassical IL-1 β secretion stimulated by P2X7 receptors is dependent on inflammasome activation and correlated with exosome release in murine macrophages. *J. Immunol.* **179,** 1913–1925.
43. Ito, Y., Kawamura, I., Kohda, C., Tsuchiya, K., Nomura, T., Mitsuyama, M. (2005) Seeligeriolysin O, a protein toxin of *Listeria seeligeri*, stimulates macrophage cytokine production via Toll-like receptors in a profile different from that induced by other bacterial ligands. *Int. Immunol.* **17,** 1597–1606.
44. Malley, R., Henneke, P., Morse, S. C., Cieslewicz, M. J., Lipsitch, M., Thompson, C. M., Kurt-Jones, E., Paton, J. C., Wessels, M. R., Golenbock, D. T. (2003) Recognition of pneumolysin by Toll-like receptor 4 confers resistance to pneumococcal infection. *Proc. Natl. Acad. Sci. USA* **100,** 1966–1971.
45. Park, J. M., Ng, V. H., Maeda, S., Rest, R. F., Karin, M. (2004) Anthrolysin O and other Gram-positive cytolysins are Toll-like receptor 4 agonists. *J. Exp. Med.* **200,** 1647–1655.
46. Srivastava, A., Henneke, P., Visintin, A., Morse, S. C., Martin, V., Watkins, C., Paton, J. C., Wessels, M. R., Golenbock, D. T., Malley, R. (2005) The apoptotic response to pneumolysin is Toll-like receptor 4 dependent and protects against pneumococcal disease. *Infect. Immun.* **73,** 6479–6487.
47. Shoma, S., Tsuchiya, K., Kawamura, I., Nomura, T., Hara, H., Uchiyama, R., Daim, S., Mitsuyama, M. (2008) Critical involvement of pneumolysin in production of interleukin-1α and caspase-1-dependent cytokines in infection with *Streptococcus pneumoniae* in vitro: a novel function of pneumolysin in caspase-1 activation. *Infect. Immun.* **76,** 1547–1557.
48. Solini, A., Chiozzi, P., Morelli, A., Fellin, R., Di Virgilio, F. (1999) Human primary fibroblasts in vitro express a purinergic P2X7 receptor coupled to ion fluxes, microvesicle formation and IL-6 release. *J. Cell Sci.* **112,** 297–305.
49. Mehta, V. B., Hart, J., Wewers, M. D. (2001) ATP-stimulated release of interleukin (IL)-1β and IL-18 requires priming by lipopolysaccharide and is independent of caspase-1 cleavage. *J. Biol. Chem.* **276,** 3820–3826.
50. Kahlenberg, J. M., Lundberg, K. C., Kertesy, S. B., Qu, Y., Dubyak, G. R. (2005) Potentiation of caspase-1 activation by the P2X7 receptor is dependent on TLR signals and requires NF-κB-driven protein synthesis. *J. Immunol.* **175,** 7611–7622.
51. Yoshikawa, H., Kawamura, I., Fujita, M., Tsukada, H., Arakawa, M., Mitsuyama, M. (1993) Membrane damage and interleukin-1 production in murine macrophages exposed to listeriolysin O. *Infect. Immun.* **61,** 1334–1339.
52. Gonzalez, M. R., Bischofberger, M., Pernot, L., van der Goot, F. G., Freche, B. (2008) Bacterial pore-forming toxins: the (w)hole story? *Cell. Mol. Life Sci.* **65,** 493–507.
53. Gurcel, L., Abrami, L., Girardin, S., Tschopp, J., van der Goot, F. G. (2006) Caspase-1 activation of lipid metabolic pathways in response to bacterial pore-forming toxins promotes cell survival. *Cell* **126,** 1135–1145.
54. Kloft, N., Busch, T., Neukirch, C., Weis, S., Boukhallouk, F., Bobkiewicz, W., Cibis, I., Bhakdi, S., Husmann, M. (2009) Pore-forming toxins activate MAPK p38 by causing loss of cellular potassium. *Biochem. Biophys. Res. Commun.* **385,** 503–506.
55. Walev, I., Reske, K., Palmer, M., Valeva, A., Bhakdi, S. (1995) Potassium-inhibited processing of IL-1 β in human monocytes. *EMBO J.* **14,** 1607–1614.
56. Bhakdi, S., Muhly, M., Korom, S., Hugo, F. (1989) Release of interleukin-1 β associated with potent cytocidal action of staphylococcal α-toxin on human monocytes. *Infect. Immun.* **57,** 3512–3519.
57. Bhakdi, S., Bayley, H., Valeva, A., Walev, I., Walker, B., Kehoe, M., Palmer, M. (1996) Staphylococcal α-toxin, streptolysin-O, and *Escherichia coli* hemolysin: prototypes of pore-forming bacterial cytolysins. *Arch. Microbiol.* **165,** 73–79.
58. Lich, J. D., Arthur, J. C., Ting, J. P. Y. (2006) Cryopyrin: in from the cold. *Immunity* **24,** 241–243.

KEY WORDS:
bacterial · cytokines · inflammation